Interaction induced AC-Stark shift of exciton-polaron resonances

T. Uto,[1,2,*] B. Evrard,[1,*] K. Watanabe,[3] T. Taniguchi,[3] M. Kroner,[1] and A. İmamoğlu[1]

[1] *Institute for Quantum Electronics, ETH Zürich, CH-8093 Zürich, Switzerland*
[2] *Institute of Industrial Science, The University of Tokyo, 4-6-1 Komaba, Meguro-ku, Tokyo 153-8505, Japan*
[3] *Research Center for Electronic and Optical Materials, NIMS, 1-1 Namiki, Tsukuba 305-0044, Japan*

Laser induced shift of atomic states due to the AC-Stark effect has played a central role in cold-atom physics and facilitated their emergence as analog quantum simulators. Here, we explore this phenomena in an atomically thin layer of semiconductor $MoSe_2$, which we embedded in a heterostructure enabling charge tunability. Shining an intense pump laser with a small detuning from the material resonances, we generate a large population of virtual collective excitations, and achieve a regime where interactions with this background population is the leading contribution to the AC-Stark shift. Using this technique we study how itinerant charges modify – and dramatically enhance – the interactions between optical excitations. In particular, our experiments show that the interaction between attractive polarons could be more than an order of magnitude stronger than those between bare excitons.

Introduction — Atomically thin transition metal dichalcogenides (TMDs) and their van der Waals heterostructures constitute a versatile platform for exploration of phenomena at the frontier of many-body physics and quantum optics [1–3]. Arguably, the most significant feature of this new platform is the weak dielectric screening and relatively heavy band-mass of electrons and holes, leading to strong Coulomb interactions and appearance of tightly bound excitons as elementary optical excitations. On the one hand, the small Bohr radius ($a_{\mathrm{ex}} \sim 1$nm) of excitons implies strong coupling to light, which ensures that a pristine monolayer TMD realizes an atomically-thin mirror in the absence of a cavity [4, 5] and exhibits large normal-mode splitting between exciton-polariton modes when embedded inside a cavity [6, 7]. On the other hand, electron- or hole-exchange based interaction between two tightly bound excitons is drastically reduced, leading to a predominantly linear optical response [5, 8, 9]. Therefore, strong exciton-photon coupling is fundamentally linked to weak exciton-exciton interactions in TMDs, which in turn constitutes a major challenge to the prospect of engineering nonlinear optical devices [10–13].

Different approaches that could meet this challenge by enhancing exciton-exciton interactions without sacrificing strong light-matter coupling have been explored. While promising results are reported [9, 14–16], the large uncertainty in the determination of the underlying exciton-exciton interaction strength has been a major hindrance in assessing and comparing these approaches. Measurement of the interaction-induced blue-shift under direct resonant excitation leads to generation of a sizeable dark exciton population, rendering the extracted interaction strength unreliable. A partial remedy is provided by studying nonlinear response of exciton-polaritons; however, recent theoretical work showed that interactions between exciton-polaritons can be drastically different from those between bare excitons [17].

In this Letter, we introduce a novel method to reliably measure exciton-exciton interactions, based on the light shift of the excitonic resonances in response to an intense red-detuned femtosecond laser pulse. Previously, the AC-Stark shift of excitons in TMDs was studied for large pump detuning [18, 19], in a regime well captured by the simple picture of a dressed two-level system, similar to that of a single atom in an off-resonant light field. For very large detunings, comparable to the band gap, the Bloch-Siegert shift becomes significant and has been observed in [20]. Here, we are interested in the opposite limit, where the pump detuning from the excitonic resonances is much smaller than the exciton binding energy: in this limit, the pump pulse generates a large population of virtual excitations that exist only during the pump-pulse duration. The interactions between this background of pump-generated virtual excitations and a test excitation produced by the probe pulse provide the dominant contribution to the light shift [21–26].

A possible avenue to enhance exciton-exciton interactions is to embed them in a two dimensional degenerate electron system (2DES). Following seminal studies on III-V quantum wells [27–29], recent work established that dynamical screening of excitons in a doped TMDs by the 2DES modifies the nature of elementary optical excitations, leading to the formation of attractive- and repulsive-exciton-polarons (AP and RP) [30–32]. Arguably, the principal result of our work is the use of the AC-Stark effect to measure the bare AP interactions as a function of n_e, where we demonstrate a dramatic enhancement of the polaron-polaron interaction, up to a factor ~ 35 as compared to interactions between bare excitons, for $n_e \leq 2 \times 10^{11}$ cm^{-2}. This behavior was theoretically predicted in [9], but was not experimentally observed.

Our experiments are performed on a monolayer $MoSe_2$ encapsulated in hBN, at cryogenic temperature ($T \lesssim 10$ K). Our setup is sketched in Fig. 1 **a**. A mode-locked

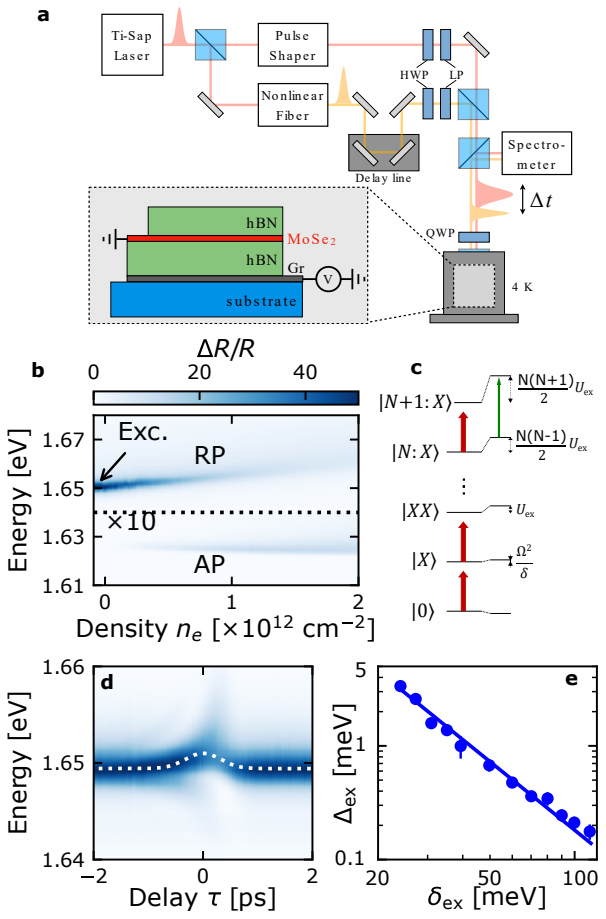

FIG. 1. **a** Sketch of the pump-probe setup and the van der Walls heterostructure. **b** Reflection spectrum of the measured device as a function of the electron density n_e. To enhance visibility, the signal is multiplied by 10 for $E < 1.64\,\mathrm{eV}$. **c** Schematic of the energy levels showing the usual AC-Stark shift for the first two-levels and the interaction induced shift which increases with the exciton density. **d** Reflection spectrum at charge neutrality, as a function of the delay between the co-circularly-polarized pump and probe pulses. From a fit (dashed line) we extract the amplitude of the light shift. The latter is shown in **e** as a function of the pump detuning from the exciton resonance (δ_{ex}), and well fitted by $\Delta_{\mathrm{ex}} = B/\delta_{\mathrm{ex}}^2$ (solid line). Throughout the manuscript, error bars show the statistical error corresponding to two standard deviations obtained from a set of a few repetitions of the experiment.

laser delivers $\sim 100\,\mathrm{fs}$ pulses. With a pulse shaper we narrow the bandwidth of the pump (increasing the duration by a factor $\lesssim 2$), while a non-linear crystal fiber generates a white-light continuum to probe the exciton and AP transition. Both pulses are focused near the diffraction limit onto the sample (more details about the sample and experimental setup in the Supplementary Material (SM) [33]).

The reflection spectrum as a function of the density n_e is shown in Fig. 1 **b**, the exciton line smoothly evolves into the RP and a red-shifted AP resonance emerges [30–32].

Exciton light shift — To benchmark our method, we first focus on the excitonic light shift at charge neutrality, for red-detuned pump laser, co-circularly polarized with the probe. For zero delay between the two pulses ($\tau = 0$) we observe a blue shift and a broadening of the exciton line (Fig. 1 **c**). The latter stems from the averaging over a spatial and time dependent light shift, since the pump and probe lasers have comparable spot size and duration. For $\tau \lesssim 0$ we also observe the emergence of weak sidebands, a common artifact of pump-probe experiments, which can be understood as the free induction decay of probe-generated excitons perturbed by the pump (for more details see *e.g.* [26, 34] or the SM [33])

For detunings $\delta_{\mathrm{ex}} = E_{\mathrm{ex}} - E_{\mathrm{pump}}$ large compared to the Rabi frequency of the pump laser (Ω_{max}), the light shift can be expanded as [23]

$$\Delta_{\mathrm{ex}} \approx \frac{A}{\delta_{\mathrm{ex}}} + \frac{B}{\delta_{\mathrm{ex}}^2}\,. \tag{1}$$

Here, the first term corresponds to the usual AC-Stark shift of a two-level system [35]. The second term arises from many-body effects, namely Coulomb interaction and Pauli blocking, due to the pump-laser-generated population of virtual excitons. These interaction effects are usually described within a Hatree-Fock approximation [24–26], in which case we can write $B/\delta_{\mathrm{ex}}^2 = U_{\mathrm{ex}} n_{\mathrm{ex}}$ where $n_{\mathrm{ex}} \propto \delta_{\mathrm{ex}}^{-2}$ is the exciton density and U_{ex} is an effective exciton-exciton interaction strength. In a regime of intermediate detunings, $\hbar\Gamma_{\mathrm{ex}}, \Omega_{max} \ll |\delta_{\mathrm{ex}}| \ll E_x$, where Γ_{ex} is the exciton radiative decay and E_x the exciton binding energy, the interaction-induced light shift is expected to dominate over the single-particle response. This is the regime explored throughout this Letter. Figure 1**d** shows that the exciton light shift is indeed well captured by a $1/\delta_{\mathrm{ex}}^2$ dependence. From this measurement we extract $U_{\mathrm{ex}} \approx 0.09 \pm 0.03\,\mu\mathrm{eV}\mu\mathrm{m}^2$ (for details on the calibration of n_{ex}, see the SM [33]). Our estimate is consistent with previous measurements [5, 8, 9], albeit an order of magnitude lower than the theoretical expectation, $\sim 3E_x a_{\mathrm{ex}}^2 \sim 1\,\mu\mathrm{eV}\mu\mathrm{m}^2$ [36, 37].

For cross-circularly polarized pump and probe lasers, producing excitons in opposite valleys, the exchange interaction is suppressed, leaving a negligible direct interaction shift [36, 37]. On the other hand, two opposit-valley excitons can bind into a biexciton. The pump drives the transition from a "probe exciton" to the biexciton, resulting in an additional contribution to the light shift, previously investigated in [38, 39]. We report similar results in the SM [33], although we point out that we obtain a biexciton binding energy $E_{\mathrm{binding}} = 29 \pm 1.5\,\mathrm{meV}$ slightly larger than the values reported in [38, 40] while being in good agreement with another recent measurement [41] (the discrepancy could stems from residual charges in ungated devices).

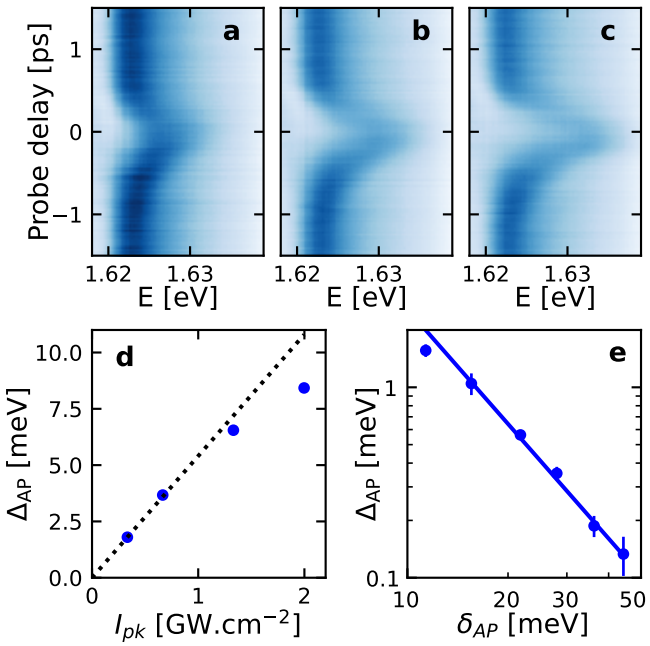

FIG. 2. AC-Stark shift of the attractive polaron (AP) resonance for co-circularly polarized pump and probe lasers. In **a-c**, we show the AP resonance as a function of the pump-probe delay τ for increasing pump laser intensity ($I_{\rm pk} \approx 0.7; 1.3; 2\,\mathrm{GW/cm^2}$). The shift at $\tau = 0$ is plotted in **d** as a function of the intensity, showing deviation from a linear dependence in $I_{\rm pk}$ (dashed line). Here the pump laser detuning from AP is $\delta_{\rm AP} \approx 13\,\mathrm{meV}$ and the electron density is $n_e \approx 1.7 \times 10^{12}\,\mathrm{cm^{-2}}$. In **e**, we show the $\delta_{\rm AP}$ dependence of the shift, which is well fitted by $B/\delta_{\rm AP}^2$, shown as a blue line. Here, $n_e \approx 0.17 \times 10^{12}\,\mathrm{cm^{-2}}$ and $I_{\rm pk} \approx 0.4\,\mathrm{GW\,cm^{-2}}$ so that the $I_{\rm pk}$ dependence is within the linear regime.

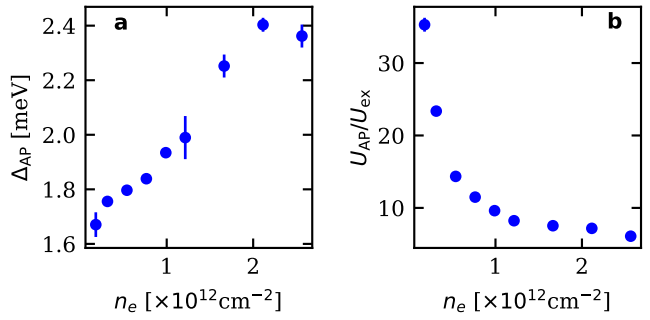

FIG. 3. **a** Electron density dependence of the attractive polaron (AP) light shift for co-circularly polarized pump and probe beam. From this data and a measurement of the AP oscillator strength [33], the AP-AP interaction strength $U_{\rm AP}$ is extracted and compared to the exciton-exciton interaction strength $U_{\rm ex}$ in **b**. Here, $\delta_{\rm AP} \approx 25\,\mathrm{meV}$ and $I_{\rm pk} \approx 1.7\,\mathrm{GW\,cm^{-2}}$.

Attractive polaron light shift — Having established our approach to measure interactions between excitons, we now turn to the main results of our paper, where we investigate the interactions between APs in an electron doped TMD. Figure 2 **a-c** shows the AP light shift for co-circularly-polarized pump and probe lasers: despite its relatively low oscillator strength ($f_{\rm AP}$), the large blue shift of the AP well exceeds its linewidth. We remark that the AP resonance is symmetric around $\tau = 0$, indicating that the pump laser does not generate incoherent AP population or quench the 2DES. This observation should be contrasted with resonant pump-probe experiments carried out using AP-polaritons [9]. However, for increasing pump intensity $I_{\rm pk}$ we observe in Fig. 2 **a-c** an overall reduction of $f_{\rm AP}$ together with a small red shift ($\approx 0.8\,\mathrm{meV}$ at most), both independent on τ. This latter observation suggests that part of the pump-pulse energy is absorbed by the TMD, which then relaxes on a time scale much longer than the pulse repetition rate. Thereby, depending on the pump intensity, we effectively change the steady-state of the TMD, presumably its temperature and/or charge density - both of which potentially leading to a reduction of $f_{\rm AP}$. As a consequence, we observe a sub-linear increase of the light shift with increasing $I_{\rm pk}$ (Fig. 2 **d**). We point out that the regime of linear dependence of $\Delta_{\rm AP}$ with $I_{\rm pk}$ increases with increasing detuning, and we are able to observe the onset of a saturation in (Fig. 2 **d**) only because the system is driven close to resonance ($\delta_{\rm AP} \approx 13\,\mathrm{meV}$). In the following we focus on a range of pump-laser detunings and intensities where the reduction of $f_{\rm AP}$ is negligible and $\Delta_{\rm AP} \propto I_{\rm pk}$.

Figure 2 **d** shows the dependence of the AP light shift on the detuning from the AP resonance ($\delta_{\rm AP} = E_{\rm AP} - E_{\rm pump}$) for $n_e \approx 0.17 \times 10^{12}\,\mathrm{cm^{-2}}$. It is well reproduced by a $\Delta_{\rm AP} \propto 1/\delta_{\rm AP}^2$ law, which demonstrates that it originates predominantly from AP-AP interactions. We point out that considering the small $f_{\rm AP}$ as compared to that of the RP oscillator strength, particularly for low n_e, one could expect that the pump generates more RP than AP (despite a smaller detuning to the latter). However, a light shift dominated by the RP population would scale as $\Delta_{\rm AP} \propto n_{\rm RP} \propto 1/\delta_{\rm RP}^2$. Even at the lowest electron densities ($n_e \approx 0.17 \times 10^{12}\mathrm{cm^{-2}}$) we measured, we do not observe such a detuning dependence and the deviation from $\Delta_{\rm AP} \propto 1/\delta_{\rm AP}^2$ law remains negligible [33]. This observation suggests that the AP-RP interactions are much weaker than the AP-AP interaction, especially for low n_e, which is consistent with the fact that the RP has a dominant exciton content in that regime.

Since $f_{\rm AP}$ increases linearly with n_e, we would normally expect $\Delta_{\rm AP}$ to also increase linearly with n_e – indeed, $\Delta_{\rm AP} = U_{\rm AP} n_{\rm AP}$ and $n_{\rm AP} \propto f_{\rm AP} \propto n_e$. At a first glance, this is indeed what we observe in fig.3 **a**. However, we also find that unlike $f_{\rm AP}$, a linear n_e fit to $\Delta_{\rm AP}$ yields a finite value for $n_e = 0$: this striking observa-

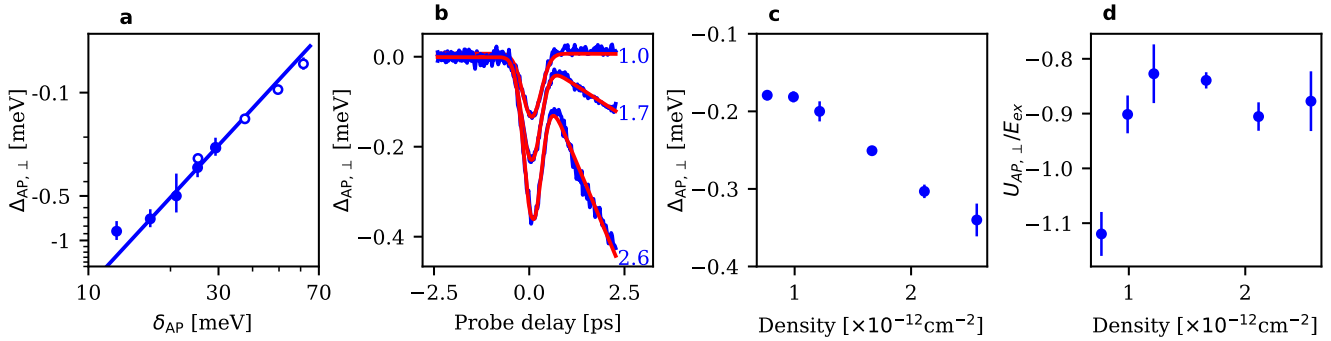

FIG. 4. Light shift of the attractive polaron (AP) for cross-circularly polarized pump and probe beam. **a** Detuning $\delta_{\rm AP}$ dependence of the light shift at an electron density of $n_e \approx 1.0 \times 10^{12}\,\mathrm{cm}^{-2}$. For large $\delta_{\rm AP}$ (open symbols) we use the full bandwidth of the pump and $I_{\rm pk} \approx 5.3\,\mathrm{GW/cm}^{-2}$. To approach the AP resonance, we reduce the bandwidth and consequently $I_{\rm pk}$ by a factor of ≈ 0.4; we then re-scale the data (full symbols), ensuring that the two measurements match at intermediate detunings ($\delta_{AP} \approx 25$; 30meV). The data is well fitted by a $B/\delta_{\rm AP}^2$ law, shown as a blue line. **b** Time dependence of the line shift for various n_e at $\delta_{\rm AP} \approx 25\,\mathrm{meV}$. The red line is a fit, from which we extract the shift at $\tau = 0$. The latter is shown in **c** as a function of n_e. **d** The ratio of the interaction between opposite valley APs and that of same valley excitons for $I_{\rm pk} \approx 1.7\,\mathrm{GW/cm}^{-2}$.

tion can be explained as an increase of the interaction strength $U_{\rm AP}$ with decreasing n_e that becomes prominent for $n_e \leq 2\times10^{11}$ cm^{-2}, where it counteracts the effect of decreasing $n_{\rm AP}$ or $f_{\rm AP}$. To highlight this feature, we compare the renormalized AP light shift $\Delta_{\rm AP}/f_{\rm AP}$ with that of the exciton $\Delta_{\rm ex}/f_{\rm ex}$, for the same pump intensity and at a wavelength such that $\delta_{\rm ex} = \delta_{\rm AP}$. In this way, we obtain the interaction ratio $U_{\rm AP}/U_{\rm ex} = \Delta_{\rm AP}/f_{\rm AP} \times f_{\rm ex}/\Delta_{\rm ex}$ which we plot in Figure 3 **b**. We observe a dramatic enhancement of the AP-AP interactions – up to a factor 35 – as n_e is lowered.

In a simple but far-reaching ansatz, the AP wavefunction is described as a superposition of a zero-momentum bare exciton plus an unperturbed 2DES, and an exciton scattered into a finite momentum state while generating a single particle-hole excitation in the 2DES of the conduction band of the opposite valley [27–30, 42]. The latter contribution could also be considered as a superposition of trion-hole pairs. For low n_e, the probability of finding a bare exciton (quasi-particle weight) in an AP excitation is small. Consequently, an AP excitation predominantly generates a collective excitation of tightly bound trions with radius $a_T \sim$ 2nm, each surrounded by a Fermi sea hole of extent on the order of the inverse Fermi wavevector k_F^{-1}. The depletion of the 2DES around the trion leads to an effective repulsive interaction between two APs, through a partial suppression of hybridization of the bare exciton and collective trion-hole excitations. The expansion of the depleted region $\propto k_F^{-1} \propto n_e^{-1/2}$ as n_e decreases can thus partially compensate for the reduction of $f_{\rm AP}$ and consequently $n_{\rm AP}$, insuring the persistence of a significant AP light shift for low n_e.

The mechanism outlined above only takes place for same-valleys APs [9, 43]. In cross-polarized configuration, we also observed an AP light shift $\Delta_{\rm AP,\perp}$, albeit much smaller in magnitude and of the opposite sign. Figure 4 **a** shows the detuning dependence of $\Delta_{\rm AP,\perp}$ which is consistent with a $\Delta_{\rm AP,\perp} \propto -1/\delta_{\rm AP}^2$ law, pointing out again to an interaction between the probe and pump laser induced APs. More importantly, we emphasize that our light shift data cannot be fitted with $\Delta_{\rm AP,\perp} \propto 1/(\delta_{AP} - E_0)$; which could have emerged from coupling to a putative charged biexciton resonance[33, 40, 43]. Figure 4 **b** shows the time dependence of the AP light shift at various densities. For $\tau > 0$ (pump before probe), we observe a continuous red shift of the AP line, which increases together with the density n_e, possibly due to residual pump-induced high momentum APs. We emphasize that this shift also exists in co-circularly-polarized pump-probe measurements but remains negligible as compared to the AC-Stark shift at $\tau = 0$. To fit the data and extract the coherent response, we use a sum of a Gaussian and a piecewise linear function. Contrary to the co-circularly-polarized case, the amplitude of the Gaussian term (coherent response) increases approximately linearly with the electron density n_e as shown in Fig. 4 **c**; here, we discarded low density $n_e < 8\times10^{12}$ cm^{-2} data for which the fit was unreliable. After proper normalization by $f_{\rm AP}$, we extract the interaction strength between opposite-valley APs, $U_{\rm AP,\perp}$, which we compare to the same-valley exciton interaction $U_{\rm ex}$ in Fig. 4 **d**: we observe almost no dependence of $U_{\rm AP,\perp}$, which remains comparable (in absolute value) to $U_{\rm ex}$ for all n_e.

To explain this observation, we consider a σ_--polarized pump laser producing APs in the K'-valley. Polaron formation promotes$K$-valley electron to high momentum

states with $k \sim 1/a_T$, thereby reducing the phase-space filling (at low k) for a probe-generated K-valley AP. For low n_E where $k_F a_T \ll 1$ this mechanism could explain the attractive interactions between opposite-valleys APs. However, further investigations are needed to confirm this hypothesis.

Conclusion and Outlook — Our work establishes the AC-Stark effect as a novel approach to measure the interaction between optical excitations in TMDs monolayers. An extension of this technique to assess the modification of interactions due to the formation of moiré heterostructures in (twisted) heterobilayers presents no difficulties. By using a detuned pump laser, we generate a large virtual exciton or AP population and thereby almost fully suppress dark-exciton generation, which plagued previous studies [9]. An exciting application of the technique we developed would rely on a Laguerre-Gauss pump beam to shift away the AP resonance, except in a small region around the beam's vortex. Increasing the pump intensity to reduce this region to a size $\sim 1/k_F$; one could use strong AP-AP interactions to generate sub-Poissonian light. For that purpose, low electron densities (small k_F) are preferable, and our finding of a persistent AP light shift in that regime is thus of paramount importance.

The data that support the findings of this Letter are available in the ETH Research Collection [44].

We are grateful to Andrea Bergschneider, Alperen Tugen, and Francesco Colangelo for their contribution to the design and fabrication of the optical setup and of the device. We also thank Feng Wang for insightful discussions. This work was supported by the Swiss National Science Foundation (SNSF) under Grant Number 200020_207520. B .E. acknowledges funding from an ETH postdoc fellowship.

---

* These authors contributed equally

[1] L. Huang, A. Krasnok, A. Alú, Y. Yu, D. Neshev, and A. E. Miroshnichenko, Reports on Progress in Physics **85**, 046401 (2022).
[2] G. Wang, A. Chernikov, M. M. Glazov, T. F. Heinz, X. Marie, T. Amand, and B. Urbaszek, Reviews of Modern Physics **90**, 021001 (2018).
[3] K. F. Mak and J. Shan, Nature Photonics **10**, 216 (2016).
[4] P. Back, S. Zeytinoglu, A. Ijaz, M. Kroner, and A. Imamoğlu, Phys. Rev. Lett. **120**, 037401 (2018).
[5] G. Scuri, Y. Zhou, A. A. High, D. S. Wild, C. Shu, K. De Greve, L. A. Jauregui, T. Taniguchi, K. Watanabe, P. Kim, *et al.*, Physical review letters **120**, 037402 (2018).
[6] X. Liu, T. Galfsky, Z. Sun, F. Xia, E. chen Lin, Y.-H. Lee, S. Kéna-Cohen, and V. M. Menon, Nature Photonics **9**, 30 (2014).
[7] N. Lundt, S. Klembt, E. Cherotchenko, S. Betzold, O. Iff, A. V. Nalitov, M. Klaas, C. P. Dietrich, A. V. Kavokin, S. Höfling, and C. Schneider, Nature Communications **7** (2016), 10.1038/ncomms13328.
[8] F. Barachati, A. Fieramosca, S. Hafezian, J. Gu, B. Chakraborty, D. Ballarini, L. Martinu, V. Menon, D. Sanvitto, and S. Kéna-Cohen, Nature nanotechnology **13**, 906 (2018).
[9] L. B. Tan, O. Cotlet, A. Bergschneider, R. Schmidt, P. Back, Y. Shimazaki, M. Kroner, and A. İmamoğlu, Physical Review X **10**, 021011 (2020).
[10] E. Shahmoon, D. S. Wild, M. D. Lukin, and S. F. Yelin, Physical Review Letters **118** (2017), 10.1103/physrevlett.118.113601.
[11] S. Zeytinoğlu, C. Roth, S. Huber, and A. İmamoğlu, Physical Review A **96** (2017), 10.1103/physreva.96.031801.
[12] A. Ryou, D. Rosser, A. Saxena, T. Fryett, and A. Majumdar, Physical Review B **97** (2018), 10.1103/physrevb.97.235307.
[13] D. S. Wild, E. Shahmoon, S. F. Yelin, and M. D. Lukin, Physical Review Letters **121** (2018), 10.1103/physrevlett.121.123606.
[14] P. Cristofolini, G. Christmann, S. I. Tsintzos, G. Deligeorgis, G. Konstantinidis, Z. Hatzopoulos, P. G. Savvidis, and J. J. Baumberg, Science **336**, 704 (2012).
[15] E. Togan, H.-T. Lim, S. Faelt, W. Wegscheider, and A. Imamoglu, Phys. Rev. Lett. **121**, 227402 (2018).
[16] I. Rosenberg, D. Liran, Y. Mazuz-Harpaz, K. West, L. Pfeiffer, and R. Rapaport, Science Advances **4** (2018), 10.1126/sciadv.aat8880.
[17] E. R. Christensen, A. Camacho-Guardian, O. Cotlet, A. Imamoglu, M. Wouters, G. M. Bruun, and I. Carusotto, "Microscopic theory of cavity-enhanced interactions of dipolaritons," (2022), arXiv:2212.02597 [cond-mat.mes-hall].
[18] J. Kim, X. Hong, C. Jin, S.-F. Shi, C.-Y. S. Chang, M.-H. Chiu, L.-J. Li, and F. Wang, Science **346**, 1205 (2014).
[19] E. J. Sie, J. W. McIver, Y.-H. Lee, L. Fu, J. Kong, and N. Gedik, Nature Materials **14**, 290 (2014).
[20] E. J. Sie, C. H. Lui, Y.-H. Lee, L. Fu, J. Kong, and N. Gedik, Science **355**, 1066 (2017).
[21] P. D. Cunningham, A. T. Hanbicki, T. L. Reinecke, K. M. McCreary, and B. T. Jonker, Nature communications **10**, 5539 (2019).
[22] A. O. Slobodeniuk, P. Koutenský, M. Bartoš, F. Trojánek, P. Malý, T. Novotný, and M. Kozák, npj 2D Materials and Applications **7** (2023), 10.1038/s41699-023-00385-1.
[23] M. Combescot, Physics reports **221**, 167 (1992).
[24] S. Schmitt-Rink and D. Chemla, Physical Review Letters **57**, 2752 (1986).
[25] R. Zimmermann, Festkörperprobleme 30: Plenary Lectures of the Divisions Semiconductor Physics Thin Films Dynamics and Statistical Physics Magnetism Metal Physics Surface Physics Low Temperature Physics Molecular Physics of the German Physical Society (DPG), Regensburg, March 26 to 30, 1990 , 295 (1990).
[26] H. Haug and S. W. Koch, *Quantum theory of the optical and electronic properties of semiconductors* (World Scientific Publishing Company, 2009).
[27] R. Rapaport, R. Harel, E. Cohen, A. Ron, E. Linder, and L. N. Pfeiffer, Physical Review Letters **84**, 1607 (2000).
[28] R. Rapaport, E. Cohen, A. Ron, E. Linder, and L. N. Pfeiffer, Physical Review B **63** (2001), 10.1103/phys-

revb.63.235310.
[29] R. A. Suris, in *Optical Properties of 2D Systems with Interacting Electrons*, edited by W. J. Ossau and R. Suris (Springer Netherlands, Dordrecht, 2003) pp. 111–124.
[30] M. Sidler, P. Back, O. Cotlet, A. Srivastava, T. Fink, M. Kroner, E. Demler, and A. Imamoglu, Nature Physics **13**, 255 (2017).
[31] D. K. Efimkin and A. H. MacDonald, Physical Review B **95**, 035417 (2017).
[32] D. Huang, K. Sampson, Y. Ni, Z. Liu, D. Liang, K. Watanabe, T. Taniguchi, H. Li, E. Martin, J. Levinsen, *et al.*, Physical Review X **13**, 011029 (2023).
[33] for more details see Supplemental Material, which includes Refs [45-51].
[34] S. Koch, N. Peyghambarian, and M. Lindberg, Journal of Physics C: Solid State Physics **21**, 5229 (1988).
[35] C. Cohen-Tannoudji and S. Reynaud, Journal of Physics B: Atomic and Molecular Physics **10**, 345 (1977).
[36] C. Ciuti, V. Savona, C. Piermarocchi, A. Quattropani, and P. Schwendimann, Physical Review B **58**, 7926 (1998).
[37] V. Shahnazaryan, I. Iorsh, I. A. Shelykh, and O. Kyriienko, Physical Review B **96**, 115409 (2017).
[38] C.-K. Yong, J. Horng, Y. Shen, H. Cai, A. Wang, C.-S. Yang, C.-K. Lin, S. Zhao, K. Watanabe, T. Taniguchi, *et al.*, Nature Physics **14**, 1092 (2018).
[39] E. J. Sie, C. H. Lui, Y.-H. Lee, J. Kong, and N. Gedik, Nano letters **16**, 7421 (2016).
[40] K. Hao, J. F. Specht, P. Nagler, L. Xu, K. Tran, A. Singh, C. K. Dass, C. Schüller, T. Korn, M. Richter, *et al.*, Nature communications **8**, 15552 (2017).
[41] L. B. Tan, O. K. Diessel, A. Popert, R. Schmidt, A. Imamoglu, and M. Kroner, arXiv preprint arXiv:2212.11145 (2022).
[42] F. Chevy, Physical Review A **74**, 063628 (2006).
[43] J. B. Muir, J. Levinsen, S. K. Earl, M. A. Conway, J. H. Cole, M. Wurdack, R. Mishra, D. J. Ing, E. Estrecho, Y. Lu, *et al.*, Nature Communications **13**, 6164 (2022).
[44] See http://hdl.handle.net/20.500.11850/614328.
[45] P. Zomer, M. Guimarães, J. Brant, N. Tombros, and B. Van Wees, Applied Physics Letters **105**, 013101 (2014).
[46] A. Laturia, M. L. Van de Put, and W. G. Vandenberghe, npj 2D Materials and Applications **2**, 6 (2018).
[47] K. K. Kim, A. Hsu, X. Jia, S. M. Kim, Y. Shi, M. Dresselhaus, T. Palacios, and J. Kong, ACS nano **6**, 8583 (2012).
[48] E. C. Regan, D. Wang, C. Jin, M. I. B. Utama, B. Gao, X. Wei, S. Zhao, W. Zhao, Z. Zhang, K. Yumigeta, M. Blei, J. D. Carlström, K. Watanabe, T. Taniguchi, S. Tongay, M. Crommie, A. Zettl, and F. Wang, Nature **579**, 359 (2020).
[49] Y. Tang, L. Li, T. Li, Y. Xu, S. Liu, K. Barmak, K. Watanabe, T. Taniguchi, A. H. MacDonald, J. Shan, and K. F. Mak, Nature **579**, 353 (2020).
[50] Y. Shimazaki, I. Schwartz, K. Watanabe, T. Taniguchi, M. Kroner, and A. Imamoğlu, Nature **580**, 472 (2020).
[51] T. Smoleński, O. Cotlet, A. Popert, P. Back, Y. Shimazaki, P. Knüppel, N. Dietler, T. Taniguchi, K. Watanabe, M. Kroner, and A. Imamoglu, Physical Review Letters **123**, 097403 (2019).